Table I. Results for Gas-Phase Self-Exchange Reactions of Metallocenes

reactants	r_0, Å[a]	r_+, Å[a]	ΔE_{in}^*,[e] kcal/mol	k_L[f]	k_{et}[g]	efficiency[h]
$MnCp_2^{0/+}$	2.04[b]	1.80[c]	8.7	1.05×10^{-9}	6.3×10^{-12}	0.006
$FeCp_2^{0/+}$	1.666[b]	1.706[b]	0.34	1.05×10^{-9}	1.3×10^{-10}	0.12
$CoCp_2^{0/+}$	1.733[b]	1.622[d]	2.5	1.04×10^{-9}	3.7×10^{-10}	0.36
$RuCp_2^{0/+}$	1.827[i]			9.0×10^{-10}	1.2×10^{-10}	0.13

[a] Estimated distances from metal to center of Cp in neutrals (r_0) and ions (r_+). [b] Reference 19. [c] Estimated from chromocene structure.[19] [d] Estimated from distances in $[(C_5H_5)(C_5H_4COOH)Co]PF_6$ (Riley, P. E.; Davis, R. E. *J. Organomet. Chem.* **1978**, *152*, 1978). [e] Estimated using $\Delta E_{in}^* = f_0 f_+ (\Delta r)^2/(f_0 + f_+)$,[6,7,24] where f_0 and f_+ are the estimated M-Cp force constants[19] and $\Delta r = r_0 - r_+$. [f] Langevin collision frequency (cm^3 $molecules^{-1}$ s^{-1}).[23] The polarizability of ferrocene was used in all cases. [g] From eq 2 in text (cm^3 $molecules^{-1}$ s^{-1}). Rates determined at ~375 K. [h] Efficiency = k_{obsd}/k_L. [i] Haaland, A.; Nilson, J. E. *Acta Chem. Scand.* **1968**, *22*, 2653.

self-exchange rate, (1), of $\sim 6 \times 10^6$ M^{-1} s^{-1} has been determined by NMR (in CD_3OD at 298 K)[11,12] and pseudo-self-exchange methods.[17,18] We have studied the gas-phase self-exchange rates for ferrocene, ruthenocene, cobaltocene, and manganocene with their corresponding cations using Fourier transform ion cyclotron resonance mass spectrometry. By use of the double resonance technique, one or more isotopes of the parent ion are ejected from the cell thereby leaving isotopically "enriched" cations to react with the neutrals present in their natural isotopic abundancies. Related ICR studies of metallocenes have been reported,[21] but the self-exchange processes were not investigated.

The ratios of the parent ion peaks were established for various reaction times and second-order rate constants were derived from eq 2, where a_0 and a_0' are the fractional natural abundancies of

$$\ln\left[\frac{R_t - (a_0'/a_0)}{R_t + 1}\right] = -k_{et}Pt \qquad (2)$$

the ejected and nonejected isotopes, respectively ($a_0 = 1 - a_0'$), R_t is the value of a'/a detected at time t after ejection, and P is the total pressure of reactants during the reaction.[22]

Results for the four metallocenes are summarized in Table I along with theoretically estimated values of the inner reorganization barrier ΔE^*_{in} and the Langevin collision rate k_L.[23] In three of the ion-neutral reactions studied here, the estimated efficiencies are somewhat lower than the maximum 0.5, but the manganocene-manganocenium reaction is substantially slower than the others.

A useful qualitative picture for the appropriate gas-phase potential energy surface for these reactions would be similar to the double-well potential used extensively by Brauman and others to interpret gas-phase nucleophilic displacement reactions[2] and proton transfers.[1a,c] The central barrier would derive from ΔE^*_{in} and the potential minima result from stabilizing ion-molecule interactions.[24]

It is possible that the much lower efficiency of the $MnCp_2^{+/0}$ self-exchange results from the relatively higher reorganizational barrier (ΔE^*_{in}) for changing the M-C bond lengths in the neutral-ion interconversion (Table I). The dimensions of the neutral metallocenes are known from gas-phase electron-diffraction studies,[19] and manganocene has unusually long M-C bonds due to its high-spin d^5 electronic configuration. Unfortunately, no crystal structure or spectroscopic data for the manganocenium ion is available, but the predicted ground state is a low-spin d^4 electronic configuration.[25]

Another possible reason for the low efficiency of the $Mn(Cp)_2^{+/0}$ self-exchange is the nature of spin multiplicities in the reactants. The direct exchange between the ^6A ground state of manganocene and the predicted ^3E or ^3A ground state[25,26] of the manganocenium ion is forbidden. The coupling of these states must rely on spin-orbit mixing with higher lying states, as described for the $[Co(NH_3)_6]^{3+/2+}$ exchange reaction[27] and spin-equilibrium processes.[28] At this point, the contribution of nonadiabaticity to the $Mn(Cp)_2^{+/0}$ reaction cannot be assessed because of the absence of spectroscopic data for the reactants.

The present results are consistent with a relatively small barrier for ferrocene, cobaltocene, and ruthenocene self-exchange due to molecular reorganization and the predominance of ΔG^*_{out} in their solution self-exchange kinetics.[15,16] For example, the rate for $FeCp_2^{+/0}$ is a factor of $\gtrsim 10^4$ faster in the absence of solvent. On the other hand, a significant contribution from ΔG^*_{in} in analogous manganocene reactions is expected. We are exploring other gas-phase redox reactions to define the proper theoretical basis for quantifying the values of ΔE^*_{in}.

Acknowledgment. This work was supported by a grant from Research Corporation (D.E.R.) and by the Office of Naval Research (J.R.E.). The Nicolet FTMS-1000 was purchased under the joint D.O.D.-University Research Instrumentation Program (J.R.E.). Ruthenocene was generously provided by Professor Henry Taube.

(20) Extensive references for individual metallocenes can be found in "Comprehensive Organometallic Chemistry"; Wilkinson, G., Stone, F. G. A., Abel, E. W., Eds.; Pergamon Press: Oxford, 1982.
(21) (a) Corderman, R. R.; Beauchamp, J. L. *Inorg. Chem.* **1976**, *15*, 665. (b) Foster, M. S.; Beauchamp, J. L. *J. Am. Chem. Soc.* **1975**, *97*, 4814.
(22) Equation 2 was derived for reversible first-order processes, and the use of ratios corrects for the decay of the ion population at longer reaction times.
(23) Gioumousis, G.; Stevenson, D. P. *J. Chem. Phys.* **1958**, *29*, 294.
(24) (a) Richardson, D. E., in preparation. (b) Drzaic, P. S.; Brauman, J. I. *J. Am. Chem. Soc.* **1982**, *104*, 13.
(25) Clack, D. W. *Theor. Chim. Acta* **1974**, *35*, 157.
(26) Robbins, J. L.; Edelstein, N. M.; Cooper, S. R.; Smart, J. C. *J. Am. Chem. Soc.* **1979**, *101*, 3853.
(27) (a) Buhks, E.; Bixon, M.; Jortner, J.; Navon, G. *Inorg. Chem.* **1979**, *18*, 2014. (b) Gesolowitz, D. Ph.D. Thesis, Stanford University, 1982.
(28) Buhks, E.; Navon, G.; Bixon, M.; Jortner, J. *J. Am. Chem. Soc.* **1980**, *102*, 2918.

Direct Measurements of Rate Differences among Nuclear Spin Sublevels in Reactions of Biradicals[1]

G. L. Closs* and O. D. Redwine

Department of Chemistry, The University of Chicago Chicago, Illinois 60637
Chemistry Division, Argonne National Laboratory Argonne, Illinois 60439

Received May 3, 1985

Ever since the formulation of the radical pair theory of CIDNP[2] it has been accepted that in radical pairs and certain biradicals different nuclear spin states may exhibit different reaction kinetics. However, direct measurements of the kinetics describing population differences of individual nuclear sublevels have never been reported, presumably because nuclear states are hard to resolve optically and NMR measurements are considered too slow to give the necessary temporal resolution. In this paper we wish to report the first such measurement employing our time-resolved CIDNP technique.[3]

(1) Supported by NSF Grant CHE 8218164.
(2) For general reviews on CIDNP, see: "Spin Polarization and Magnetic Effects in Radical Reactions"; Molin, Yu, N., Ed.; Elsevier: Amsterdam, 1984. "Chemically Induced Magnetic Polarizationσqt; Muus, L. T., Atkins, P. W., McLauchlan, K. A., Pedersen, J. B., Eds.; Reidel: Dordrecht, 1977. Freed, J. H.; Pedersen, J. B. *Adv. Magn. Reson.* **1976**, *8*, 1. Closs, G. L. *Adv. Magn. Reson.* **1974**, *7*, 157.

0002-7863/85/1507-6131$01.50/0

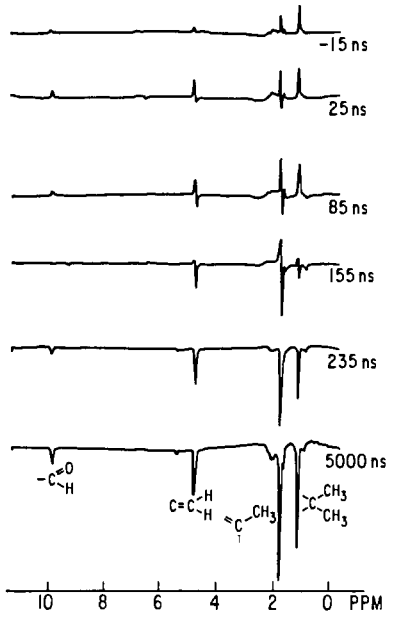

Figure 1. NMR spectra (60-MHz) obtained on photolysis of **1** after the indicated delay τ, which is measured from the laser pulse to the center of the rf pulse. The finite width of the rf pulse accounts for negative τ. The origin of the signals are labeled according to the protons in **1** and **3**.

Different reaction rates for molecules in different nuclear substates imply changes in line intensities in the product NMR spectra during the course of the reaction. The first example of this is shown in Figure 1 picturing the 60-MHz spectra obtained on laser flash photolysis of 2,2-dimethylcyclooctanone (**1**) as function of the delay τ between laser excitation and radio frequency (rf) probing pulses. During the first 200 ns the spectra change dramatically from absorption to emission with some absorption–emission multiplets in between. The products, **1** and the enal **3**, are formed from the intermediate biradical **2** according to the scheme

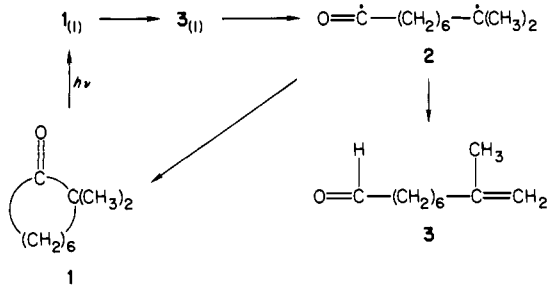

A qualitative understanding of the spectra is provided by the following considerations. The biradical is initially formed in its triplet state (T)[4] which mixes with the singlet (S) by hyperfine (hf) interaction and Zeeman energy differences ($\Delta g\beta B_0$). It is known[5] that the average singlet energy of a 1,8-biradical lies between the T_0 and T_- state at the reaction field (1.4 T) and is closer to T_0 than T_-. The largest energy gap is between S and T_+. At the beginning of the reaction the stronger T_0–S mixing causes a radical pair type spectrum which for the magnetic parameters of **2** ($\Delta g > 0$, hf coupling $a < 0$) should be all absorption (Kaptein's rule).[6] However, in contrast to what happens in radical pairs, the T_0–S spectrum will disappear entirely when T_0 nuclear

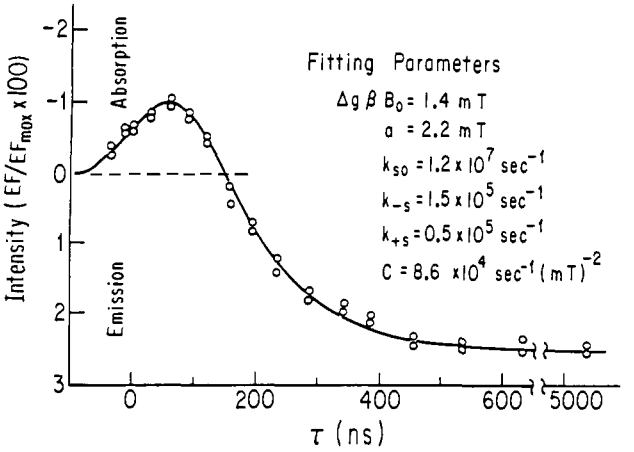

Figure 2. Best fit to experimental points (O) of the intensity of the *gem*-dimethyl resonance of **1**. A deconvolution method was used for the calculated curve to correct for the finite rf pulse width. Within the assumptions inherent in the model the parameters listed give a unique fit and their errors are estimated as less than 20%.

levels with smaller mixing coefficients have caught up with their faster counterparts in crossing to S. Since there is no nuclear spin flip and no diffusive separation, all T_0 sublevels get converted to the corresponding S states. So, considering only T_0 and S, one would predict an absorptive spectrum to grow in and then to fade away within a very short time. In contrast, $T_\pm$–S crossings are accompanied by nuclear spin flips ($\Delta m = \pm 1$) and can produce a lasting all emissive or absorptive pattern. The superposition of T_0–S and $T_\pm$–S crossings leads to the time evolution shown in Figure 1 if mixing with T_0 predominates and mixing with T_- is more important than with T_+.

We have modeled the kinetics for a biradical with six identical protons ($I = 3$) using g factors and hf constants from closely related systems.[7] At first sight this appears to involve 10 unknowns, k_{so}, a nuclear spin independent rate constant such as caused by spin orbit coupling, $k_\pm$, the rate constants for the crossing from the $T_\pm$ levels to the appropriate S states, and the seven rate constants k_{om} ($m = I, I-1, I-2, \ldots, -I$) connecting the T_0 sublevels with the identical levels in S. Fortunately, the ratios of these seven constants are fixed by the known hf and g values, making use of the relationship[8]

$$k_{om} = C(\Delta g\beta B_0 + am)^2$$

Also, k_{so}, k_{+s}, and k_{-s} are interrelated via the experimentally determined absolute intensity at the infinity point ($\tau > 1$ μs). The problem can be reduced to a three-parameter fit, two determining the shape of the intensity–τ curve and the third its scale, by assuming the ratio k_{+s}/k_{-s} to be given by the ratio of the squares of the average mixing coefficients at the reaction field.[9] The best fit for the *gem*-dimethyl signal of **1** is shown in Figure 2 obtained with the parameters listed. The total exit rate constants for the individual substates of T are ($k_{so} + k_{om}$) for T_0 and ($K_{so} + (I \mp m)k_\pm$) for $T_\pm$.[10]

The results are noteworthy in two respects. First, the predominant rate is nuclear spin independent (k_{so}) causing the low

(3) Miller, R. J.; Closs, G. L. *Rev. Sci. Instrum.* **1981**, *52*, 1876. Closs, G. L.; Redwine, O. D. *J. Am. Chem. Soc.* **1985**, *107*, 4543. Closs, G. L.; Miller, R. J.; Redwine, O. D. *Acc. Chem. Res.*, in press.

(4) Heine, H. G.; Hartman, W.; Kory, D. R.; Magyar, J. G.; Hoyle, E. C.; McVey, J. K.; Lewis, F. D. *J. Org. Chem.* **1974**, *39*, 691.

(5) Closs, G. L.; Doubleday, C., Jr. *J. Am. Chem. Soc.* **1972**, *94*, 9248; **1973**, *95*, 2735. Closs, G. L. *Adv. Magn. Reson.* **1974**, *7*, 157.

(6) Kaptein, R. *J. Chem. Soc. D* **1971**, 732.

(7) Landolt-Börnstein, **1977**, *9b*, 181.

(8) In radical pair CIDNP, degenerate T_0–S levels, it is the frequency of the oscillations of the diagonal elements of the density matrix that determines the time evolution of the wave function. With a large energy mismatch between S and T levels as in biradicals this frequency becomes very large but the amplitudes are quite small and control intersystem crossing. The amplitudes are determined by the squares of the mixing coefficients which are proportional to the right-hand side of the equation.

(9) For an average singlet–triplet splitting of 0.38 T[5] and a reaction field of 1.4 T the ratio of the squares of the energy differences between S and T_+ and S and T_- is 3.0. The ratio of the mixing coefficients is the inverse of that number.

(10) In a flexible biradical as **2** the singlet–triplet splitting varies with the conformation. As a consequence all rate constants are conformation- and thus time-dependent. Our model does not take this into consideration.

intensity of the infinity spectrum (2.5% of the theoretical maximum).[11] This has a leveling effect on the influence of the nuclear spin dependence on the total exit rate for each biradical sublevel although differences as large as 30% remain. Next, the nuclear spin dependent rates are relatively slow [(3×10^4)–(3×10^6) s^{-1}]. This is the result of the poor energy match of S with the T levels. In radical pairs T_0 and S can become degenerate and spin dependent rate constants may be as large as 10^8 s^{-1}. The parameters of Figure 2 also reproduce nicely the absorption–emission features observed for **3** if a negative nuclear spin coupling constant is assumed. The origin of this multiplet effect lies in the interplay of T_0–S and $T_\pm$–S mixing and is fundamentally different from that observed in radical pairs.

Cyclooctanone shows qualitatively the same behavior, first a T_0–S spectrum followed by a predominant T_-–S pattern. However, cycloheptanone is emissive at all times signifying predominant T_-–S mixing as expected for the larger singlet–triplet splitting in a shorter biradical. Of course, the patterns observed will depend strongly on the magnitude of the reaction field because the Zeeman splitting determines the relative weight of the mixing of S with the three T levels.

In summary, we have shown here by a direct kinetic method that molecules identical in all parts of their wave function except the nuclear spin component can react with measurably different rates.

(11) The theoretical maximum of the infinity spectrum is obtained by setting $k_{+s} << K_{-s} >> k_{so}$.

Improved Energy Storage in a Two-Polyelectrolyte System

Richard E. Sassoon*

Energy Research Center and Department of Physical Chemistry, Hebrew University of Jerusalem Jerusalem 91904, Israel

Received June 3, 1985

A major goal in photochemical solar energy conversion systems involving photoinduced-electron-transfer reactions is the inhibition of the reverse-electron-transfer reaction regenerating the ground-state reactants. This may then allow useful chemical reactions to occur yielding photochemical fuels. Attempts to retard the back-electron-transfer reaction have usually been made by adding a suitable microenvironment such as micelles,[1] vesicles,[2] microemulsions,[3] charged colloids,[4] or polyelectrolytes[5-12] to the system. For example, in the presence of appropriate polyelectrolytes the yields of photoinduced-electron-transfer products may be enhanced and their rates of reverse electron transfer retarded in photochemical systems containing polypyridyl derivatives of ruthenium together with ferricyanide,[6,7] a zwitterionic viologen derivative,[8] and various polyviologens.[9,10] In this paper a new two-polyelectrolyte system is described in which isolation of the two final photochemical products on separate similarly charged polyelectrolytes leads to a very much greater reduction in their rate of reverse electron transfer than observed previously.

Earlier work in this laboratory has shown that reactive radical species can be very greatly stabilized when they are formed on highly charged polyelectrolytes.[13] For example, the rate of radical–radical dimerization reactions for radicals formed by hydrogen atom abstraction of quarternary ammonium cations, which usually occur close to the diffusion-controlled rate, may be inhibited by about 5 orders of magnitude when they are formed on the polyelectrolyte polybrene (repeating unit: $\{[-(CH_2)_6N(CH_3)_2(CH_2)_3N(CH_3)_2-]^{2+}(F^-)_2\}$). This impressive reduction in rate was attributed to both the low ability of stretched polyelectrolytes to diffuse through solution and the high electrostatic repulsion of their positive charges.

Application of this result to attain stabilization of photochemical-electron-transfer products was achieved in this work by covalently bonding a photosensitizer molecule and a donor molecule to separate positive polyelectrolytes. The polyelectrolyte-linked photosensitizer I consisted of a tris(2,2′-bipyridine)ruthenium

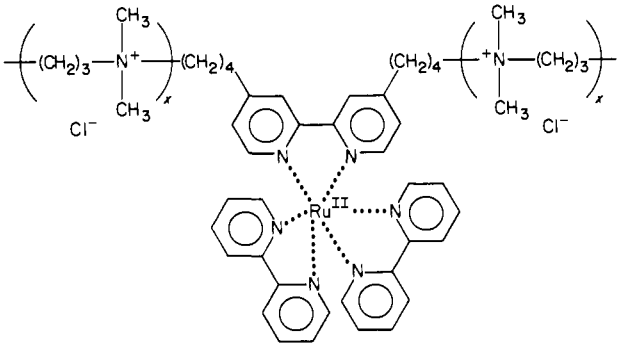

I

derivative linked to a poly(3,3-ionene) polyelectrolyte while the polyelectrolyte-linked donor molecule II contained an *N,N,N′*,-

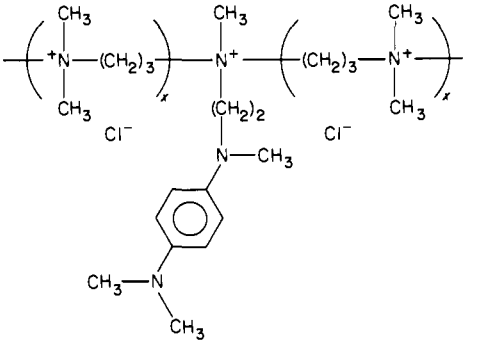

II

N′-tetraalkyl-*p*-phenylenediamine derivative linked to a similar polyelectrolyte. A mediator species is necessary to allow generation of the two-polyelectrolyte-linked redox products and the compound chosen was 4-methoxy-*N,N*-dimethylaniline (MeODMA) which possesses the appropriate redox potential for this electron-transfer system.[14]

Following excitation of I by light of wavelength 450 nm (eq 1) quenching of its lowest emitting excited state occurs with a

$$I \xrightarrow{h\nu} I^* \quad (1)$$

$$I^* + MeODMA \rightarrow I^- + MeODMA^+ \quad (2)$$

$$I^- + MeODMA^+ \rightarrow I + MeODMA \quad (3)$$

$$MeODMA^+ + II \rightarrow MeODMA + II^+ \quad (4)$$

$$I^- + II^+ \rightarrow I + II \quad (5)$$

* Present Address: Radiation Laboratory, University of Notre Dame, Notre Dame, IN 46556.

(1) (a) Brugger, P.-A.; Infelta, P. P.; Braun, A. M.; Grätzel, M. *J. Am. Chem. Soc.* **1981**, *103*, 320. (b) Brugger, P.-A.; Grätzel, M.; Guarr, T.; McLendon, G. *J. Phys. Chem.* **1982**, *86*, 944.
(2) Fang, Y.; Tollin, G. *Photochem. Photobiol.* **1983**, *38*, 429.
(3) Kiwi, J.; Grätzel, M. *J. Am. Chem. Soc.* **1978**, *100*, 6314.
(4) Willner, I.; Yang, J.-M.; Laane, C.; Otvos, J. W.; Calvin, M. *J. Phys. Chem.* **1981**, *85*, 3277.
(5) Rabani, J.; Sassoon, R. E. *J. Photochem.* **1985**, *29*, 7.
(6) Sassoon, R. E.; Rabani, J. *J. Phys. Chem.* **1980**, *84*, 1319.
(7) Sassoon, R. E.; Rabani, J., *J. Phys. Chem.*, in press.
(8) (a) Sassoon, R. E.; Rabani, J. *Isr. J. Chem.* **1982**, *22*, 138. (b) Sassoon, R. E.; Aizenshtat, Z.; Rabani, J. *J. Phys. Chem.* **1985**, *89*, 1182.
(9) Lee, P. C.; Matheson, M. S.; Meisel, D. *Isr. J. Chem.* **1982**, *22*, 133.
(10) Sassoon, R. E.; Gershuni, S.; Rabani, J. *J. Phys. Chem.* **1985**, *89*, 1937.
(11) Itoh, Y.; Morishima, Y.; Nozakura, S.-I. *Photochem. Photobiol.* **1984**, *39*, 603.
(12) Morishima, Y.; Itoh, Y.; Nozakura, S.-I.; Ohno, T.; Kato, S. *Macromolecules*, **1984**, *17*, 2264.
(13) Sassoon, R. E.; Rabani, J. *J. Phys. Chem.* **1984**, *88*, 6389.
(14) Bock, C. R.; Connor, J. A.; Gutierrez, A. R.; Meyer, T. J.; Whitten, D. G.; Sullivan, B. P.; Nagle, J. K. *J. Am. Chem. Soc.* **1979**, *101*, 4815.

0002-7863/85/1507-6133$01.50/0